Absolute rate coefficient of the reaction of CF$_2$(ã ^{3}B$_1$) with O$_2$ between 288 and 600 K

Bart Dils,* Shaun Avondale Carl and Jozef Peeters

*Department of Chemistry, University of Leuven, Celestijnenlaan 200F, B-3001, Leuven, Belgium.
E-mail: Bart.Dils@chem.kuleuven.ac.be, Shaun.Carl@chem.kuleuven.ac.be and
Jozef.Peeters@chem.kuleuven.ac.be*

The rate coefficient of the removal of electronically excited CF$_2$(ã ^{3}B$_1$) by O$_2$ (quenching as well as reaction) has been determined for the first time over an extended temperature range (288–600 K). CF$_2$(^{3}B$_1$) radicals were generated by pulsed laser photolysis of C$_2$F$_4$ at 193 nm and real-time pseudo-first-order decays of the relative CF$_2$(^{3}B$_1$) concentration were obtained by monitoring the CF$_2$(^{3}B$_1$ → ^{1}A$_1$) emission at 570–700 nm. This new CF$_2$(^{3}B$_1$)-generation technique allows a straightforward determination of the absolute rate constants. Over the experimental temperature range, the rate coefficient exhibits a simple Arrhenius behaviour with a small activation energy, described by: $k_{\text{oxygen}}(T) = (6.7 \pm 1.9) \times 10^{-12}$ exp$[-(200 \pm 100)\text{K}/T]$ cm^3 s^{-1} molecule^{-1}. No pressure dependence was observed over the 1–20 Torr range using He as the bath gas.

Introduction

Fluorocarbon radicals are of major importance in the chemistry of plasmas used for semiconductor etching in electronic device processing. In-depth knowledge of the relevant gas-phase reactions of the various active plasma species is required for a quantitative understanding of the controlling processes in plasma etching. Much research has been performed on the reactivity of various fluorocarbon radicals such as CF,[1] CF$_3$ [2] and CF$_2$(X̃ ^{1}A$_1$).[3–7] One of the most notable features of CF and CF$_2$(^{1}A$_1$) is that they both have a vacant π-orbital/lone pair combination on the carbon atom. This orbital structure normally leads to a high reactivity, in particular towards bond insertion reactions. However, in the case of halocarbons, the C atom electron deficiency is largely quenched through back donation by the lone pairs of the halogen atom. Among the halocarbons this effect is the strongest for F atoms due to the comparable size of fluorine and carbon, which facilitates orbital overlap. In the case of CF$_2$(^{1}A$_1$) the effects of back donation are so drastic that the carbene is hardly reactive at all, save for the notable exception of the reaction with O (see Table 1), and is stabilised to such an extent that CF$_2$(^{1}A$_1$) is the ground state (as opposed to excited state CH$_2$(ã ^{1}A$_1$)) lying 56.6 kcal mol^{-1} [8] below the triplet excited CF$_2$(ã ^{3}B$_1$) state. CF$_2$(^{3}B$_1$) is a biradical and is therefore believed to be far more

reactive than its ground state. This, combined with a relatively long radiative lifetime of about 1 s [9] (note that Young *et al.*[10] contest these findings) and the distinct possibility of substantial CF$_2$(^{3}B$_1$) formation in halocarbon etching plasmas, either directly or through reactions C + CF$_3$ → CF$_2$(^{3}B$_1$) + CF [11] and *via* energy transfer between N$_2$(A $^3\Sigma_u^+$) and CF$_2$(^{1}A$_1$),[12] might make CF$_2$(^{3}B$_1$) a key player in plasma etching systems.
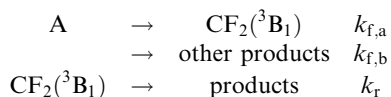
Literature data on the electronically excited triplet difluoromethylene radical, CF$_2$(^{3}B$_1$), are extremely scarce. Most research regarding CF$_2$(^{3}B$_1$) has focussed on its generation by the C$_2$F$_4$ + O(^{3}P) reaction[8,10,13–15] and not so much on the reactivity of CF$_2$(^{3}B$_1$) itself. There is still substantial debate concerning the CF$_2$(^{3}B$_1$) yield of the above reaction ($\leq$1%,[10] 80% [16] or 85% [13] depending on the source). Directly linked with the yield (η) is the radiative lifetime of CF$_2$(^{3}B$_1$), determined to range between 0.19η and 4η s.[9] As far as the authors are aware, only two groups have reported extensively on the reactivity of CF$_2$(^{3}B$_1$), both studies being limited to room temperature measurements. Koda [9] examined the CF$_2$(^{3}B$_1$) phosphorescence emission produced in N$_2$O–Hg–C$_2$F$_4$ mixtures following irradiation with a low-pressure mercury lamp. The time-resolved emission showed a first-order decay soon after an initial rise. In the given conditions, the decay constant corresponded to the bimolecular rate constant for the C$_2$F$_4$ + O(^{3}P) reaction. The rate coefficients of CF$_2$(^{3}B$_1$) removal by various other species were obtained by examining the decrease of the emission intensity upon addition of these coreactants. Dodonov *et al.*[17] analysed the CF$_2$(^{3}B$_1$) kinetics using threshold ionisation mass spectrometry to distinguish CF$_2$(^{3}B$_1$) from ground state CF$_2$(^{1}A$_1$). The total rate of CF$_2$(^{3}B$_1$) decay was determined by numerical modelling of the relative concentration evolution of CF$_2$(^{3}B$_1$) radicals using a complex reaction scheme and fitting to experimental data. Although Young *et al.*[10] focussed primarily on the determination of the yield of CF$_2$(^{3}B$_1$) in the C$_2$F$_4$ + O(^{3}P) reaction system, they found the CF$_2$(^{3}B$_1$) removal rate constants with O$_2$ to be about ten times less than those found by Koda.[9] This observation played a key role in their conclusion of precursor involvement in the reaction system.

Table 1 Published bimolecular rate coefficient values at room temperature for various CF$_2$(^{1}A$_1$) reactions

X	k(CF$_2$(^{1}A$_1$) + X)/cm^3 s^{-1} molecule^{-1}	Ref.
O$_2$	$< 8.3 \times 10^{-18}$	3
O	$(1.63 \pm 0.3) \times 10^{-11}$	4
NO	$3.5 \times 10^{-32\,a}$	5
C$_2$H$_4$	$< 8.30 \times 10^{-16}$	6
C$_2$F$_4$	$< 4.98 \times 10^{-18}$	7

^{a} Derived from the Arrhenius equation obtained over a 1600 to 2500 K temperature range and should be treated merely as an indication.

A more elegant way to determine the $CF_2(^3B_1)$ rate coefficients would be to work under pseudo-first order conditions and simply derive the removal rate directly from the exponential decays of the $CF_2(^3B_1 \rightarrow {}^1A_1)$ emission for various coreactant concentrations. This method however is preferably used under conditions where the total rate of $CF_2(^3B_1)$ removal is (far) less than that of its generation. Under these conditions the single-exponential decay at longer reaction times will correspond to the rate of $CF_2(^3B_1)$ radical removal, which greatly facilitates analysis and enhances accuracy. The concentration *vs.* time evolution of $CF_2(^3B_1)$ in the following reaction mechanism

$$
\begin{array}{rcll}
A & \rightarrow & CF_2(^3B_1) & k_{f,a} \\
 & \rightarrow & \text{other products} & k_{f,b} \\
CF_2(^3B_1) & \rightarrow & \text{products} & k_r
\end{array}
$$

$$[CF_2(^3B_1)](t) = \left(\frac{k_{f,a}[A]_0}{k_r - k_f}\right)(\exp(-k_f t) - \exp(-k_r t))$$

is described by the expression that over time will evolve into a simple first-order decay given by

$$\lim_{t \to \infty}[CF_2(^3B_1)](t) = \left(\frac{k_{f,a}[A]_0}{k_r - k_f}\right)(\exp(-k_s t))$$

where k_s is the smallest of k_f and k_r. When the overall rate of [A] removal, k_f, is larger than the rate of $CF_2(^3B_1)$ removal, k_r, the decay at longer times will correspond with the rate of overall removal of $CF_2(^3B_1)$. Under these conditions information on the reactivity of $CF_2(^3B_1)$ is contained in the final part of the emission profile and thus will be generally easy to quantify accurately.

Using the $C_2F_4 + O(^3P)$ reaction as a source for $CF_2(^3B_1)$, as did Koda [9] and Dodonov *et al.*,[17] the preferred conditions whereby the rate of $CF_2(^3B_1)$ removal is less than the decay rate of its precursor A, are hard to establish. Since the bimolecular rate constant of the $C_2F_4 + O$ reaction, $(7.1 \pm 0.2) \times 10^{-13} \text{ cm}^3 \text{ s}^{-1} \text{ molecule}^{-1}$ at room temperature,[9] is relatively low compared to the rate constants of subsequent $CF_2(^3B_1)$ removal by various species such as $O(^3P)$ $[(3.4 \pm 1) \times 10^{-11} \text{ cm}^3 \text{ s}^{-1} \text{ molecule}^{-1}]$[17] and O_2 $[(4.1 \pm 0.8) \times 10^{-12} \text{ cm}^3 \text{ s}^{-1} \text{ molecule}^{-1}]$,[9] and barely twice as large as the rate constant for removal of $CF_2(^3B_1)$ by C_2F_4 itself $[(3.9 \pm 0.8) \times 10^{-13} \text{ cm}^3 \text{ s}^{-1} \text{ molecule}^{-1}]$,[9] very large concentrations of C_2F_4 and only trace amounts of $O(^3P)$ would be required to meet the favoured experimental conditions.

Minton *et al.*[18] have demonstrated that the dissociation of C_2F_4 by 193 nm radiation follows two decomposition pathways, both involving C=C double-bond breaking. One channel leads to two ground state singlet $CF_2(^1A_1)$ products while the other correlates with the formation of one ground-state $CF_2(^1A_1)$ fragment and one excited-state triplet $CF_2(^3B_1)$ fragment. Their observed 470–700 nm spectrum proved to be virtually identical to the spectrum previously assigned to $CF_2(^3B_1)$ phosphorescence in the reaction of C_2F_4 with $O(^3P)$.[8,14] The 193 nm photolysis of C_2F_4 was used as $CF_2(^3B_1)$ generation process in our present experiments; contrary to the less suited $C_2F_4 + O(^3P)$ reaction, it allows us to carry out $CF_2(^3B_1)$ kinetics measurements in the preferred conditions outlined above.

Instrumental setup

a. Apparatus

The apparatus (Fig. 1) is part of a Pulsed Laser Photodissociation/Laser Induced Fluorescence (PLP/LIF) setup described earlier.[1,19] Electronically excited $CF_2(^3B_1)$ radicals were generated pulsewise by 193 nm photodissociation of C_2F_4 using the output of an ArF excimer laser (EMG 101 MSC, Lambda Physik) with the beam collimated to a diameter of 0.5 cm to
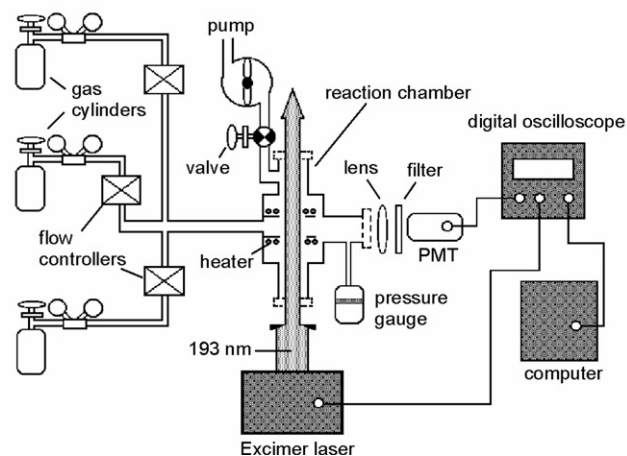

Fig. 1 Schematic diagram of experimental setup.

eliminate beam–wall interaction. The pulse duration is ≈ 20 ns; the repetition frequency was 2 Hz, and the pulse energy ≈ 5 mJ. The 470–720 nm $CF_2(^3B_1 \rightarrow {}^1A_1)$ emission [8] from the reaction region was passed through a > 570 nm long-pass filter and detected by a Hamamatsu 1P28 photomultiplier. The PM voltage supply was gated to suppress the signal over the first 100 µs after the laser pulse to eliminate the intense short-lived window fluorescence excited by the 193 nm excimer laser beam, before the signal was collected by a digital (PICO ADC200, 100 MHz) oscilloscope and stored on a PC for analysis.

The blackened stainless steel reaction cell is resistively heatable up to a temperature of 1000 K. However, the present experiments were constrained to the range $T \leq 600$ K due to the radiation of the heating coils in the $\lambda \geq 570$ nm region of interest. The temperature in the observed reaction volume ($20 \text{ mm}^2 \times ca.$ 10 mm) was measured by a movable calibrated chromel/alumel thermocouple. While always positioned in the heatable reaction cell, once a stable temperature was obtained, the thermocouple was pulled back from the reaction volume to avoid interaction with the laserbeam. All experiments, except those exploring the pressure dependence, were carried out at a total pressure of 20 Torr, measured by a Datametrics Barocel sensor. He 99.9996% purity (UCAR), used as bath gas, and O_2 99.995% purity (L'Air Liquide), were obtained commercially. C_2F_4 of the highest grade (min 99.9% pure, confirmed by a mass spectrometric scan) was provided to us by Dyneon Research, Germany. The flow rates of the gases were regulated and measured by calibrated mass flow controllers (MKS). The concentration of the species in the reaction cell were determined from the fractional flows, the total pressure and the temperature. The total gas flow was sufficiently large to refresh the gas in the observed volume between successive laser shots.

b. Method

A rough stepwise spectrum (resolution = 10 nm, step-size = 10 nm) of the transient emission in the 470–700 nm region, is shown in Fig. 2 and comparison with the spectra taken by Koda[8] and Zhou *et al.*[14] (both in stationary state systems and using high resolution scans), showed that the observed emission had all the distinct features of the $CF_2(^3B_1 \rightarrow {}^1A_1)$ emission, confirming the results from Minton *et al.*[18]

The time evolution of $CF_2(^3B_1)$ was monitored by its luminescence $I(CF_2(^3B_1))$ for $\lambda > 570$ nm. The rapid vibrational quenching of $CF_2(^3B_1)$ by He $[k = (9.3 \pm 4.6) \, 10^{-13} \text{ cm}^3 \text{ s}^{-1} \text{ molecule}^{-1};$[20] *i.e.* $\tau_{rel} \approx 1.7$ µs at 20 Torr] precludes possible interference of this process in the determination of the $CF_2(^3B_1)$ removal kinetics, with a time scale of thousands of µs. The concentration of the reactant O_2 was in large excess over $[CF_2(^3B_1)]$ such that the kinetics were pseudo-first-order. To
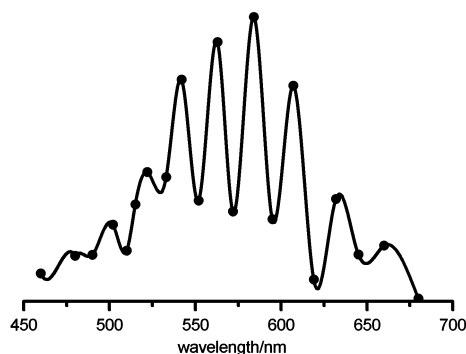
Fig. 2 Rough stepwise spectrum of the $CF_2(^3B_1 \rightarrow {}^1A_1)$ emission, data-points connected with a cubic spline function. The maxima and minima correspond perfectly with the $CF_2(^3B_1 \rightarrow {}^1A_1)$ spectrum obtained by Zhou et al.[14] and Koda[8] in the 520–680 nm range.

eliminate all traces of non-$CF_2(^3B_1)$ emission a background emission signal was obtained by eliminating all C_2F_4 from the reaction system. All recorded $I(t)$ traces were corrected for the background trace, in identical conditions (except [C_2F_4]). The first-order decay constants (k') at a given temperature were measured under fixed conditions of total pressure, [C_2F_4] and total flow-rate. Only the concentration of the reactant O_2, always in large excess, was varied. Plots of k' as a function of reagent concentration [O_2] yield a straight line with a slope equal to the rate constant of interest and an intercept equal to the sum of the rates of all other $CF_2(^3B_1)$ loss processes such as diffusion, convection, radiative decay and quenching with species such as He and C_2F_4, all of which are fixed for the full set of experiments at a given temperature.

Results

Fig. 3 represents a typical emission *vs.* time profile of $CF_2(^3B_1)$. The profile could only be fitted by a tri-exponential equation for a system of three consecutive first order reactions, obeying the expression:

$$I(t) = k_1 k_2 A \left[\frac{\exp(-k_1 t)}{((k_2 - k_1)(k_3 - k_1))} + \frac{\exp(-k_2 t)}{((k_1 - k_2)(k_3 - k_2))} + \frac{\exp(-k_3 t)}{((k_1 - k_3)(k_2 - k_3))} \right]$$
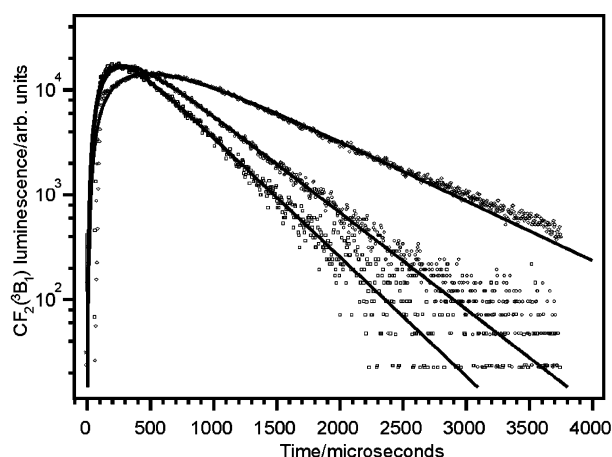

Fig. 3 Time evolution and corresponding fits of the CF_2-$(^3B_1) \rightarrow CF_2(^1A_1)$ luminescence intensity upon 193 nm pulsed irradiation of 1.6×10^{15} molecules cm^{-3} C_2F_4 at 20 Torr and $T = 295$ K for various concentrations O_2 (0.0×10^{14}, 1.9×10^{14} and 4.5×10^{14} molecules cm^{-3}) with He as bath gas.

This strongly indicates that the formation path involves at least two intermediates before resulting in $CF_2(^3B_1)$. In light of the non-zero anisotropy parameter ($\beta = -0.2$) for photofragments resulting from the photodissociation of C_2F_4 at 193 nm obtained by Minton at al.,[18] it seems that the initially excited $C_2F_4^*$ does not possess a sufficiently long lifetime to be regarded as one of the long-lived intermediates. However, to explain the deviation from pure isotropy ($\beta = -1.0$) Minton et al.[18] suggested the possibility of simultaneous excitation of C_2F_4 to its excited singlet and triplet states, only one of which dissociating instantaneously. The above suggests that the $CF_2(^3B_1)$ formation mechanism from the dissociation of C_2F_4 by 193 nm radiation is more complex than that proposed by Minton et al.,[18] a possibility which these authors did not exclude in their article.

The initial conversion rates k_1 and k_2 ranged typically from 7000 to 15 000 s^{-1} and 14 000 to 20 000 s^{-1} respectively. Note that the obtained rate coefficients k_1, k_2 and k_3 are mathematically indistinguishable; re-assigning the obtained values to different ks would yield an identically shaped curve, save for a change in magnitude. There is no doubt however that the removal rate of $CF_2(^3B_1)$, k_3, can be assigned to the lowest obtained k, belonging to the well defined decay part of the $CF_2(^3B_1)$ emission signal, as the other rate constants are too large to be explained by current known $CF_2(^3B_1)$-removal rates with He [$(4.2 \pm 2) \times 10^{-15}$ cm^3 s^{-1} molecule^{-1}][17] and C_2F_4 [$(3.9 \pm 0.8) \times 10^{-13}$ cm^3 s^{-1} molecule^{-1}].[9]

Furthermore, although it was difficult to obtain a clear picture of the influence of various parameters (pressure, [O_2]) on the two rate coefficients embedded in the rise of the tri-exponential curve, due to the larger errors imposed upon them by the uncertainties of the growth part of the $CF_2(^3B_1)$ emission signal, we were able to deduce the influence of O_2 on the lowest of the two, obtaining a bimolecular rate coefficient equal to $(2.5 \pm 1) \times 10^{-11}$ cm^3 s^{-1} molecule^{-1}. (No clear temperature dependence was observed.) This coefficient is considerably larger than values obtained by Koda [$(4.1 \pm 0.8) \times 10^{-12}$ cm^3 s^{-1} molecule^{-1}][9] and Young et al. [$\sim 4 \times 10^{-13}$ cm^3 s^{-1} molecule^{-1}][10] for the $CF_2(^3B_1) + O_2$ rate coefficient.

The decay rates attributed to $CF_2(^3B_1)$ were derived from the tri-exponential fits and plotted as a function of [O_2] (see examples in Fig. 4). The gradients of these plots represent the absolute bimolecular rate coefficients k_3. The rate coefficients were determined at eight temperatures between 288 and 600 K and are listed in Table 2. An Arrhenius representation is displayed in Fig. 5. The combined repeatability and statistical errors of the present k determinations were typically between 4 and 8%, except for the 600 K measurement where they were 10% due to the increased background radiation from the heating coils. The stated errors in Table 2 amounting to about 15% (30% for the 600 K measurement), include estimated possible systematic errors that could result from
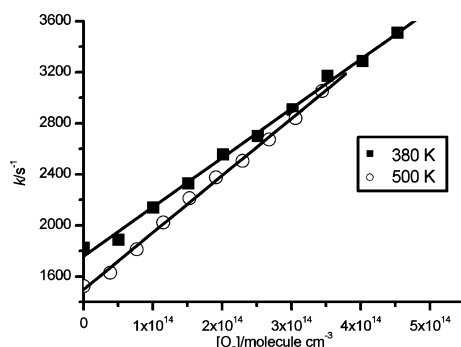

Fig. 4 Plot of the obtained decay rate constants at 380 and 500 K in function of [O_2]. The slope yields the values of $k(CF_2(^3B_1) + O_2)$ for the respective temperatures. The relatively small changes in the intercept stem from the influence of temperature on the He concentration.

Table 2 Bimolecular rate coefficients k_{oxygen} for the $CF_2(^3B_1)$ removal by O_2 from this work

T/K	$1000T^{-1}/K^{-1}$	$k_{oxygen}/cm^3\ s^{-1}\ molecule^{-1}$
288	3.47	$(3.2 \pm 0.5) \times 10^{-12}$
295	3.39	$(3.5 \pm 0.5) \times 10^{-12}$
325	3.08	$(3.6 \pm 0.5) \times 10^{-12}$
350	2.86	$(3.8 \pm 0.6) \times 10^{-12}$
380	2.63	$(3.9 \pm 0.6) \times 10^{-12}$
425	2.35	$(4.3 \pm 0.6) \times 10^{-12}$
500	2.00	$(4.5 \pm 0.7) \times 10^{-12}$
600	1.67	$(4.6 \pm 1.4) \times 10^{-12}$

Table 3 Bimolecular rate coefficients k_{oxygen} for the $CF_2(^3B_1)$ removal by O_2 in function of total pressure, at 295 K

P/Torr	$k_{oxygen}/cm^3\ s^{-1}\ molecule^{-1}$
1	$(3.2 \pm 0.9) \times 10^{-12}$
10	$(3.8 \pm 0.6) \times 10^{-12}$
20	$(3.5 \pm 0.5) \times 10^{-12}$

inaccuracies in the absolute reactant concentrations and other experimental parameters.

Pressure dependence measurements have been performed between 1 and 20 Torr and the data are listed in Table 3. No significant pressure influence has been observed.

Discussion and conclusions

The room temperature data of the bimolecular rate coefficient of $CF_2(^3B_1) + O_2$ is in good agreement with the result obtained by Koda [$(4.1 \pm 0.8) \times 10^{-12}$ cm^3 s^{-1} molecule^{-1}].[9] The temperature dependence follows a simple Arrhenius form and can be expressed by $k(T) = (6.7 \pm 1.9) \times 10^{-12}$ exp$[-(200 \pm 100)K/T]$ cm^3 s^{-1} molecule^{-1}. Our compatibility with Koda's results imply our disagreement with the results of Young *et al.*[10]

The magnitude of the rate constant and the absence of a marked temperature dependence are indicative of a radical–radical combination reaction as the (only) rate-controlling step. The absence of pressure dependence shows that the initial combination products do not redissociate back into reactants, but either (isomerise and) dissociate into final products, or are collisionally stabilised. The $CF_2(^3B_1) + O_2$ combination can either yield (i) an (activated) singlet carbonyloxide $F_2COO(S)^\dagger$, which is strongly stabilised by resonances ($\Delta H_f^\circ(298) = -60$ kcal mol^{-1},[21] *vs.* the reactants $\Delta H_f^\circ(298) = 10$ kcal mol^{-1} [8,22]), or (ii) an (activated) triplet diradical, $F_2\dot{C}O\dot{O}(T)^\dagger$, which can be estimated to lie only 35 kcal mol^{-1} below the reactants (assuming a $F_2\dot{C}$–$O\dot{O}$ bond energy similar to that in F_3C–$O\dot{O}$).[23]

$$CF_2(^3B_1) + O_2(^3\Sigma_u) \rightarrow F_2COO(S) \quad \Delta_r H = -70\ \text{kcal mol}^{-1}$$
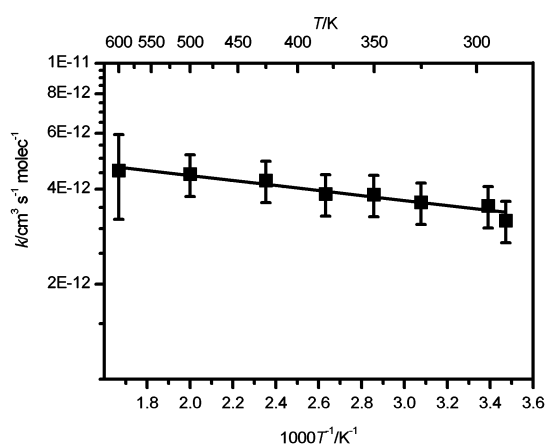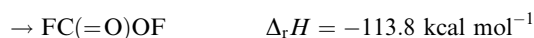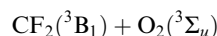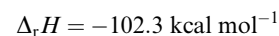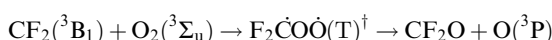$$CF_2(^3B_1) + O_2(^3\Sigma_u) \rightarrow F_2\dot{C}O\dot{O}(T) \quad \Delta_r H \cong -35\ \text{kcal mol}^{-1}$$

Fig. 5 Plot of the temperature dependence of $k(CF_2(^3B_1) + O_2)$ and corresponding Arrhenius fit. Note that the uncertainties of each data-point includes estimations of systematic errors. These errors should be similar for each experiment.

The first, $F_2COO(S)^\dagger$, with a nascent internal energy of $\cong 70$ kcal mol^{-1}, is unlikely to yield $CF_2O + O(^1D)$, as the product potential energy ($\sum \Delta_f H = -46.8$ kcal mol^{-1}) lies well above the transition state ($\Delta_f H = -50$ kcal mol^{-1}) for isomerisation to the very low-lying difluorodioxirane c-$F_2CO_2^\dagger$ ($\Delta_f H = -102 \pm 1.5$ kcal mol^{-1}), as calculated by Kraka *et al.*[21] This highly activated c-$F_2CO_2^\dagger$ may undergo collisional stabilisation at high pressures, or, at lower pressures, it can further isomerise to difluorodioxymethane $F_2C(\dot{O})\dot{O}$ and/or to $FC(=O)OF$ ($\Delta_f H = -103.6$ kcal mol^{-1}),[21] which may then ultimately dissociate into $F + F + CO_2$, $F_2 + CO_2$, $FCO + OF$, among others. When stabilised, c-$F_2CO_2^\dagger$ may undergo mutual reaction, which has been suggested to lead to $2\ CF_2O + O_2$.[23] Thus the following overall channels may occur on the singlet surface:

$$CF_2(^3B_1) + O_2(^3\Sigma_u)$$
$$\rightarrow \text{c-}CF_2O_2(\text{dioxirane}) \quad \Delta_r H = -112.2\ \text{kcal mol}^{-1}$$
$$\rightarrow CO_2 + F_2 \quad \Delta_r H = -104.2\ \text{kcal mol}^{-1}$$
$$\rightarrow FCO + OF \quad \Delta_r H = -25.2\ \text{kcal mol}^{-1}$$
$$\rightarrow CO_2 + 2F \quad \Delta_r H = -66.3\ \text{kcal mol}^{-1}$$
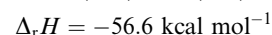$$\rightarrow FC(=O)OF \quad \Delta_r H = -113.8\ \text{kcal mol}^{-1}$$

Alternatively, in the presence of added olefins, the stabilized c-$F_2CO_2^\dagger$ may oxidize these to regio- and stereoselective (ep)oxidation products, as suggested by Rahman *et al.*[24] to explain their observations in $C/CF_4/O_2$ systems with added olefinic trapping agents.

The fate of the activated triplet $F_2\dot{C}O\dot{O}^\dagger$ is less clear. One possible reaction path leads to the formation of CF_2O through

$$CF_2(^3B_1) + O_2(^3\Sigma_u) \rightarrow F_2\dot{C}O\dot{O}(T)^\dagger \rightarrow CF_2O + O(^3P)$$
$$\Delta_r H = -102.3\ \text{kcal mol}^{-1}$$

The C_2F_4/O experiments ($P_{tot} > 500$ Torr) performed by Heicklen *et al.*[13] did show a pronounced increase in the CF_2O concentration when adding O_2; it was this increase that led them to conclude that $CF_2(^3B_1)$ is formed in the $C_2F_4 + O(^3P)$ reaction, estimating a yield of 85%. However, they attributed this increase to a short chain: $CF_2O_2 + C_2F_4 \rightarrow 2CF_2O + CF_2(^3B_1)$ $CF_2(^3B_1) + O_2 \rightarrow CF_2O_2$, in which the chain carrier CF_2O_2 – the precise nature of which was not specified – is removed by either $2CF_2O_2 \rightarrow 2CF_2O + O_2$ or $CF_2O_2 + C_2F_4 \rightarrow CF_2O + C_2F_4O$. Furthermore, free O atoms are not expected to yield the stereospecific olefinic oxidation products observed by Rahman *et al.*[24] The $F_2\dot{C}O\dot{O}(T)^\dagger \rightarrow CF_2O + O(^3P)$ dissociation may have to face an appreciable energy barrier, and could be outrun by a more facile process:

$$CF_2(^3B_1) + O_2(^3\Sigma_u) \rightarrow F_2\dot{C}O\dot{O}(T)^\dagger \rightarrow CF_2(^1A_1) + O_2(^3\Sigma_u)$$
$$\Delta_r H = -56.6\ \text{kcal mol}^{-1}$$

which, overall, amounts to "physical" quenching of $CF_2(^3B_1)$ to its singlet ground state $CF_2(^1A_1)$. Finally, it cannot be entirely excluded that the barriers of the two potential $F_2\dot{C}O\dot{O}(T)$ reactions discussed above are so high that all nascent $F_2\dot{C}O\dot{O}(T)^\dagger$ biradicals redissociate back into the reactants at low to moderate pressures. If so, only the reaction on the

singlet surface would be effective (*i.e.* lead to products) at such pressures. Based on the known low- and high-pressure rate constants of the similar reaction[25] of

$$CF_3 + O_2 \rightleftharpoons CF_3O_2^{\dagger} \xrightarrow{M} CF_3O_2,$$
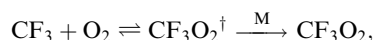
the rate of redissociation of the activated $F_2\dot{C}O\dot{O}(T)$ to $CF_2 + O_2$ can be estimated to be of the order of $(1–10) \times 10^8$ s^{-1}, over our pressure range of 1–20 Torr He, this would result in an increase of the collisional stabilisation fraction from *ca.* 0.25–2.5% to 5–35%, which is not incompatible with our total k_{oxygen}-data as a function of pressure. At a pressure of 1 atm, the stabilisation fraction should then approach 90%, and the total k_{oxygen} should accordingly be significantly higher. However this could not be verified experimentally, since at higher pressures the $CF_2(^3B_1)$ removal is dominated entirely by quenching by the bath gas, and as the $CF_2(^3B_1 \rightarrow {}^1A_1)$ emission becomes far too weak. Beside experimental product studies, additional theoretical studies, in particular on triplet CF_2O_2 should be most helpful to resolve these issues.

Finally, it may be noted that the rate constant k_{oxygen} found for $CF_2(^3B_1) + O_2$ is comparable to the 295 K values of 1.6×10^{-12} cm^3 s^{-1} molecule^{-1}, reported earlier by us, for the $CF(X^2\Pi) + O_2$ reaction[1] and 3.2×10^{-12} cm^3 s^{-1} molecule^{-1} for the $CH_2 + O_2$ reaction,[26] which both were argued to proceed similarly through an activated combination product $FCOO^{\dagger}$ [1] and $CH_2OO^{\dagger}$ [27] respectively, that subsequently decomposes.

Further research regarding the reactivity of $CF_2(^3B_1)$ towards NO, H$_2$, F$_2$, ... is underway.

References

1 See, for example: J. Peeters, J. Van Hoeymissen, S. Vanhaelemeersch and D. Vermeylen, *J. Phys. Chem.*, 1992, **96**, 1257.
2 See, for example: E. W. Kaiser, T. J. Wallington and M. D. Hurley, *Int. J. Chem. Kinet.*, 1995, **27**, 205.
3 W. Hack, M. Wagner and K. Hoyermann, *J. Phys. Chem.*, 1995, **99**, 10847.
4 K. Yamasaki, A. Tanaka, A. Watanabe, K. Yokoyama and I. Tokue, *J. Phys. Chem.*, 1995, **99**, 15086.
5 A. P. Modica, *J. Chem. Phys.*, 1967, **46**, 3663.
6 J. Edelbuttel-Einhaus, K. Hoyermann, G. Rohde and H. Gg. Wagner, *Ber. Bunsen-Ges. Phys. Chem.*, 1989, **93**, 1413.
7 F. W. Dalby, *J. Chem. Phys.*, 1964, **41**, 2297.
8 S. Koda, *Chem. Phys. Lett.*, 1978, **55**, 353.
9 S. Koda, *J. Phys. Chem.*, 1979, **83**, 2065.
10 R. A. Young, J. Blauer, R. Bower and C. L. Lin, *J. Chem. Phys.*, 1988, **88**, 4834.
11 M. Rahman, M. L. McKee and P. B. Shevlin, *J. Am. Chem. Soc.*, 1986, **108**, 6296.
12 K. Yamasaki, A. Tanaka, I. Tokue and Y. Ito, *Chem. Phys. Lett.*, 1993, **215**, 483.
13 J. Heicklen, *Adv. Photochem.*, 1969, **7**, 57 and references cited therein.
14 S. Zhou, M. Zhan, Y. Qiu and S. Liu, *Chem. Phys. Lett.*, 1985, **121**, 395.
15 D. S. Y. Hsu and M. C. Lin, *Chem. Phys.*, 1977, **21**, 235.
16 A. F. Dodonov, V. V. Zelenov and A. S. Kukui, *Sov. J. Chem. Phys.*, 1990, **6**, 3368.
17 A. F. Dodonov, V. V. Zelenov and A. S. Kukui, *Sov. J. Chem. Phys.*, 1991, **7**, 1089.
18 T. K. Minton, P. Felder, R. C. Scales and J. R. Huber, *Chem. Phys. Lett.*, 1989, **164**, 113.
19 J. Peeters, S. Vanhaelemeersch, J. Van Hoeymissen, R. Borms and D. Vermeylen, *J. Phys. Chem.*, 1989, **93**, 3892.
20 S. Koda, *Chem. Phys.*, 1982, **66**, 383.
21 E. Kraka, Z. Konkoli, D. Cremer, J. Fowler and H. F. Schaefer III, *J. Am. Chem. Soc.*, 1996, **118**, 10595.
22 R. Atkinson, D. L. Baulch, R. A. Cox, R. F. Hampson, J. A. Kerr, M. J. Rossi and J. Troe, *J. Phys. Chem. Ref. Data*, 1997, **26**, 1329.
23 P. D. Lightfoot, R. A. Cox, J. N. Crowley, M. Destriau, G. D. Hayman, M. E. Jenkin, G. K. Moortgat and F. Zabel, *Atmos. Environ.*, 1992, **26A**, 1805.
24 M. Rahman, M. L. McKee, P. B. Shevlin and R. Sztyrbicka, *J. Am. Chem. Soc.*, 1988, **110**, 4002.
25 R. Atkinson, D. L. Baulch, R. A. Cox, R. F. Hampson, J. A. Kerr, M. J. Rossi and J. Troe, *J. Phys. Chem. Ref. Data*, 1997, **26**, 521.
26 D. L. Baulch, C. J. Cobos, R. A. Cox, P. Frank, G. Hayman, Th. Just, J. A. Kerr, T. Murrells, M. J. Pilling, J. Troe, R. W. Walker and J. Warnatz, *J. Phys. Chem. Ref. Data*, 1994, **23**, 847.
27 R. A. Alvarez and C. B. Moore, *J. Phys. Chem.*, 1994, **98**, 174.